Label-Free and Real-Time Detection of Tuberculosis in Human Urine Samples Using a Nanophotonic Point-of-Care Platform

Patricia Ramirez-Priego,[†] Daan Martens,[‡,§] Ayssar A. Elamin,[∥] Pieterjan Soetaert,[⊥] Wim Van Roy,[#] Rita Vos,[#] Birgit Anton,[∇] Ronny Bockstaele,[⊥] Holger Becker,[∇] Mahavir Singh,[∥] Peter Bienstman,[‡,§] and Laura M. Lechuga*,[†]

[†]Nanobiosensors and Bioanalytical Applications Group, Catalan Institute of Nanoscience and Nanotechnology (ICN2), CSIC, BIST and CIBER-BBN, Campus UAB, Bellaterra, 08193 Barcelona, Spain

[‡]Photonics Research Group, Ghent University/imec, Technologiepark-Zwijnaarde 15, 9052 Ghent, Belgium

[§]Center for Nano- and Biophotonics, Ghent University, Technologiepark-Zwijnaarde 15, 9052 Ghent, Belgium

[∥]LIONEX Diagnostics and Therapeutics GmbH, Salzdahlumer Str. 196, Building 1A, 38126 Braunschweig, Germany

[⊥]Trinean NV, Dulle-Grietlaan 17/3, 9050 Ghent, Belgium

[#]imec, Kapeldreef 75, 3001 Leuven, Belgium

[∇]microfluidic ChipShop GmbH, Stockholmer Str. 20, 07747 Jena, Germany

Ⓢ Supporting Information

ABSTRACT: Tuberculosis (TB) is the leading global cause of death from a single infectious agent. Registered incidence rates are low, especially in low-resource countries with weak health systems, due to the disadvantages of current diagnostic techniques. A major effort is directed to develop a point-of-care (POC) platform to reduce TB deaths with a prompt and reliable low-cost technique. In the frame of the European POCKET Project, a novel POC platform for the direct and noninvasive detection of TB in human urine was developed. The photonic sensor chip is integrated in a disposable cartridge and is based on a highly sensitive Mach−Zehnder Interferometer (MZI) transducer combined with an on-chip spectral filter. The required elements for the readout are integrated in an instrument prototype, which allows real-time monitoring and data processing. In this work, the novel POC platform has been employed for the direct detection of lipoarabinomannan (LAM), a lipopolysaccharide found in the mycobacterium cell wall. After the optimization of several parameters, a limit of detection of 475 pg/mL (27.14 pM) was achieved using a direct immunoassay in undiluted human urine in less than 15 min. A final validation of the technique was performed using 20 clinical samples from TB patients and healthy donors, allowing the detection of TB in people regardless of HIV coinfection. The results show excellent correlation to those obtained with standard techniques. These promising results demonstrate the high sensitivity, specificity and applicability of our novel POC platform, which could be used during routine check-ups in developing countries.

KEYWORDS: point-of-care, nanophotonic biosensor, LAM, biomarker, urine, diagnosis, tuberculosis
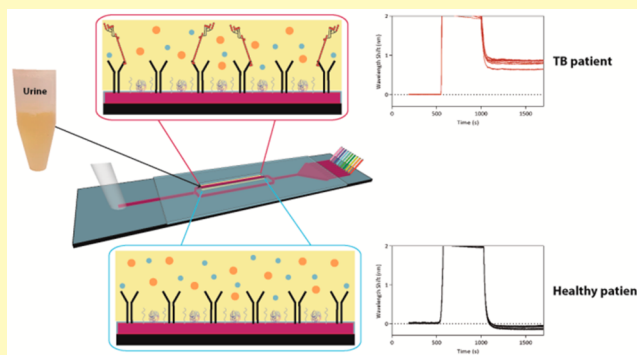
Tuberculosis (TB) is a re-emerging infectious disease caused by *Mycobacterium tuberculosis* affecting millions of people worldwide. According to the 2017 World Health Organization (WHO) report,[1] TB infected 10.4 million people, resulting in 1.7 million deaths with more than 95% of these cases occurring in developing countries. TB is considered the leading fatal infectious agent, surpassing human immunodeficiency virus (HIV) and acquired immune deficiency syndrome (AIDS).[1] Two types of TB have been identified: active and latent. In both cases, the bacterium is present in the human body. In active TB, the bacterium is constantly multiplying, invading diverse organs with a high infective potential. On the other hand, latent TB is asymptomatic and the bacterium is inactive without the ability to infect others.

Traditional methods for the detection of active TB include culture testing as the current reference standard and sputum smear microscopy. However, both of them are imprecise, slow and require qualified personnel and laboratory equipment.[1−3] Since 2010, WHO began to recommend the use of a new

molecular assay, GeneXpert (Cepheid, US), based on nucleic acid amplification for the detection of *M. tuberculosis* and for the determination of its resistance to rifampicin, the common antibiotic employed to treat several infectious diseases, including TB.[1,4] Although promising at the beginning, GeneXpert has not improved the TB screening capabilities as compared to conventional tests; also it incurs infrastructure limitations in developing countries, as it needs a controlled temperature environment, with the addition of the instrumentation, reagents, and cartridges costs.[1,5] Therefore, there is still an urgent need to develop a highly sensitive and specific point-of-care (POC) platform for the rapid diagnosis of TB in low-resource countries; a platform that should be cost efficient, user-friendly, noninvasive and requiring minimal biosafety standards.[6−8]

Several *M. tuberculosis* secreted antigens have been described as biomarkers in TB, such as lipoarabinomannan (LAM), antigen 85 complex (Ag85), ESAT-6, CFP-10, MPT64, and 38 kDa antigen.[7,9−12] These antigens can be used for the direct detection of active TB in different biological samples other than sputum, such as urine and plasma. Of these, urine is potentially the best candidate for a POC analysis as it can be readily obtained from children and adults, can be easily stored, has a low infection risk during sample collection, and does not require a laboratory with a high biosafety level.[7,13,14]

LAM is a widely known and structurally important 17.5 kDa lipopolysaccharide found in mycobacterial cell walls.[13,15−17] When *M. tuberculosis* is lysed by the host immune system, it is filtered by the kidneys and LAM can then be detected in the urine.[16] Since no human glycosidases are known for the degradation of LAM, an antigen with glycosidic linkages, it is a key potential biomarker in urine.[14] Several studies have confirmed the presence of LAM antigens in the urine of patients with active TB[13,18] and have found that the amount of LAM in urine is correlated with the bacterial burden metabolic activity and rate of degradation of the bacteria, and hence allows for a semiquantitative assessment of the infection. It has also been found that LAM antigens play a key role in phagocyte evasion,[18] modulation of the host response during infection,[19] inhibition of mycobacterial antigen processing,[18] production of tumor necrosis factor,[18] and growth and pathogenesis of *M. tuberculosis*.[20] Detection of LAM in urine has several advantages in comparison to the conventional techniques. There are ELISA and lateral flow tests commercially available for the detection of LAM in urine[15,21] with adequate diagnostic specificity of 98−99%,[22] but unsatisfactory low sensitivity for TB patients who do not have HIV. These techniques achieve higher sensitivity (61−67%) for people with less than 50 cluster of differentiation four (CD4) cells/μL, who are seriously ill HIV-positive patients, than for patients only infected with TB (4−8%).[15,22] Taking into account that TB is the leading cause of death of HIV-positive people with more than 40% of incidents worldwide[1] and that the current methods are not able to detect TB in people without HIV,[21] effort is necessary to develop new methodologies for TB diagnosis in patients with and without HIV in order to reduce the number of TB cases and deaths, especially in developing countries.

We present the optimization and validation of a novel POC platform for the direct and noninvasive detection of TB in human urine. This new POC platform was developed in the frame of a European project (www.pocket-proj.eu), and the complete description of the new instrument can be found in ref

23. The photonic sensor chip is based on a highly sensitive Mach−Zehnder Interferometer (MZI) transducer combined with an on-chip spectral filter (see Figure 1).[24] The
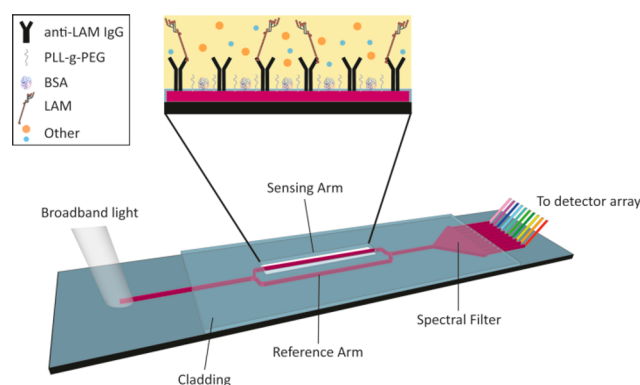

Figure 1. Layout of the photonic sensor chip based on Mach−Zehnder Interferometer transducers and readout by an on-chip spectral filter. Zoom in the sensing area shows a scheme of the biosensing interaction of the anti-LAM/LAM immunoreagents.

photonic sensor chip is integrated in a disposable polymer microfluidic cartridge. A superluminiscent diode (SLED) is used as the light source whereas a CMOS sensor is employed for the signal readout, both of which are integrated in the instrument prototype. This instrument also incorporates a pumping unit and a graphical user interface that allows real-time monitoring, data processing and controlling of fluid injection into the sensor cartridge. Prior to use, the sensor surface is functionalized with high-quality and selective monoclonal antibodies against LAM. Using this platform, TB detection is achieved in undiluted human urine samples in less than 15 min by employing a direct immunoassay. This demonstrates the high sensitivity, specificity and applicability of our platform for TB diagnosis surpassing the existing limitations of the current systems.

■ MATERIALS AND METHODS

Biological Samples. Stored urine samples from Tanzania were used for the validation of TB diagnosis technique. Twenty urine samples were used for this study, including 10 healthy donors, 5 TB patients with HIV, and 5 TB patients without HIV. All samples were previously analyzed using GeneXpert (Cepheid, US) and sputum smear microscopy.

Prototype Instrument. The photonic sensor chip (7.16 × 6.76 mm) is fabricated in silicon nitride at wafer-scale in a clean room facility, and it integrates six MZI sensors and a reference sensor (see Figure 2A). The reference sensor is used to compensate the
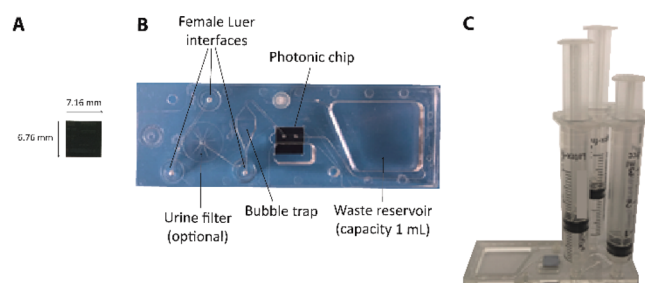

Figure 2. (A) Photonic sensor chip. (B) Microfluidic cartridge integrated with the photonic sensor chip. (C) Microfluidic cartridge employing three-syringe system.

dispersion of the grating couplers, the light source, and the on-chip spectral filter, resulting in an accuracy increase of the response.

A complete description of the new POC instrument can be found in ref 23. Briefly, a SLED (850 nm) broadband light source is coupled to each sensor simultaneously using a separated grating coupler. The output of each MZI sensor is connected to an arrayed waveguide grating (AWG) with 30 channels which work as on-chip spectral filter. Other separated grating couplers are used to couple the light from the 30 output channels of the AWG to a CMOS camera which monitors the intensity of the different spectral channels simultaneously.

The photonic sensor chip was placed in a disposable cartridge (75.5 × 25.5 mm) which is fabricated with cyclic olefin copolymer (COC) as shown in Figure 2B. The input and output grating couplers are left exposed to avoid variations in the optical pathways. A microfluidic channel delivers the sample onto the MZI sensing arms. A waste reservoir able to handle a maximum volume of 1 mL is connected at the end of the fluidic path. The cartridge includes three female Luer interfaces to facilitate connections with standard syringes employed for the injection of urine samples and the required buffers. The fluidic system includes a special bubble trap to avoid undesired air bubbles, and an optional urine filter (5 μm pore size).

The complete instrument (22 × 22 × 49.30 cm) contains the optical system, the pumping units and a touch screen as a user interface, as shown in Figure S-1. The sensors are evaluated by measuring wavelength shifts due to surface refractive index changes.

The sensorgram of each sensor is graphically displayed in real-time providing the user with immediate feedback of the patient sample diagnosis. Additionally, the interface enables the control of the pump speed and time of injection for each syringe and bubble trap monitoring.

Due to the volume limitations of the cartridge waste reservoir and the three-syringe configuration in the final POC configuration (Figure 2C), we decided to modify the instrument with an in-flow system in order to perform its complete analytical characterization at the laboratory level, prior to the evaluation of the final POC instrument. To include this in-flow system, we have added (i) a syringe pump (NewEra, US) with adjustable pumping speed, (ii) a two-position valve (VICI, US) that allows sequential loading of the sample loop and injection into the cartridge, and (iii) three Teflon caps to provide connections to the cartridge female Luer interfaces. One of these caps allows the flow of the solution in the cartridge, and the other two form a vacuum to avoid air bubbles. The evaluation of real samples with the new POC platform was performed using both the in-flow and the three-syringe configuration.

Antibody Immobilization and Direct Immunoassay. For the detection of LAM, a monoclonal IgG antibody against LAM (anti-LAM) was developed within the framework of the project by LIONEX GmbH (Germany). The antibody was diluted in PBS 10 mM and immobilized by physical adsorption onto the surface of the photonic sensor chip, followed by a blocking step to avoid nonspecific adsorptions. Milli-Q water was used as the running buffer at a flow rate of 10 μL/min.

Once the immobilization process was completed, an immunoassay was performed which allows the direct detection of LAM from the sample. The running buffer was changed to PBS 10 mM. In order to obtain a complete calibration curve, different LAM concentrations (1, 10, 50, 100, 250, 500, 750, and 1000 ng/mL) were employed. An additive assay was performed by flowing successive dilutions of increasing LAM concentrations.

RESULTS AND DISCUSSION

Evaluation of the Bulk Sensitivity. The estimation of the bulk sensitivity of the photonic sensor chip to changes in the refractive indices of a solution over its sensing area provides a preliminary evaluation of the performance and reproducibility of our device and the prototype instrument.

In order to analyze the performance of the photonic sensor chip, different solutions of PBS (5, 10, 25, 50, 75, and 100 mM), which do not chemically modify the sensor surface, were

sequentially injected providing minute changes in their refractive indices in contrast with the Milli-Q water employed as running buffer ($\Delta\eta_{PBS5mM} = 1 \times 10^{-3}$ RIU, $\Delta\eta_{PBS10mM} = 1.70 \times 10^{-3}$ RIU, $\Delta\eta_{PBS25mM} = 4.50 \times 10^{-3}$ RIU, $\Delta\eta_{PBS50mM} = 8.20 \times 10^{-3}$ RIU, $\Delta\eta_{PBS75mM} = 1.21 \times 10^{-2}$ RIU, $\Delta\eta_{PBS100mM} = 1.56 \times 10^{-2}$ RIU) (see Figure 3). The refractive indices from
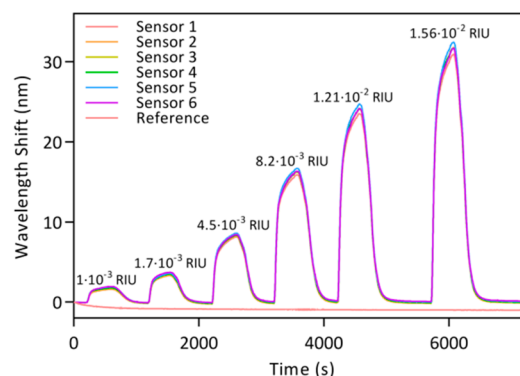

Figure 3. Calibration curve of the photonic sensor chips by flowing solutions of PBS with different refractive indices. The top of each bulk change specifies the $\Delta\eta$ that is evaluated ($\eta_{[PBS]} - \eta_{H_2O}$).

the different PBS concentrations were determined with a digital refractometer (Rudolph Research Analytical, US). The noise of the system was very low (0.003 nm) and was determined as the standard deviation of a blank signal in which only running buffer was flowing.

A linear dependence is observed in Figure 3 between the refractive index change and the measured wavelength shift variation of the sensor output. The calibration for the bulk refractive index changes was fitted to a linear model ($R^2 = 0.99$), resulting in a limit of detection (LOD) as low as 3×10^{-6} RIU. This evaluation was repeated using different sensor cartridges, and it resulted in the same LOD, demonstrating in this way the excellent performance and reproducibility of the photonic sensor chips and the POC platform.

Production of Anti-LAM and LAM. The proprietary mouse anti-LAM IgG is specific monoclonal antibody to mycobacterial LAM with high affinity toward *M. tuberculosis* LAM. Antibodies were obtained by mice immunization protocol.

The antibody was purified from defined hybridoma cells culture by affinity chromatography. The quantity of antibody was determined using the Lowry protein assay, and the purity of the antibody was analyzed using SDS gel electrophoresis, Western blotting, Tapestation, and exclusion chromatography. The antibody preparation purity was determined to be 95% pure. Specific antigen–antibody binding was determined by Western blot utilizing purified *M. tuberculosis* LAM (LIONEX, Germany) (Figure S-2) and ELISA.

Furthermore, Bio-Layer Interferometry (BLI) was used for binding affinity measurement of the purified antibody to the purified *M. tuberculosis* LAM. Our data reveals that anti-LAM IgG has low KD values (below 10^{-8} M) which indicates that this antibody possesses high affinity toward mycobacterial LAM (Figure S-3 and Table S-1). The affinity values support the high specificity and affinity of this antibody to LAM molecules.

Label-Free Immunoassay for LAM Detection. A standard physical adsorption functionalization in which the antibody is adsorbed onto the photonic sensor chip via

intermolecular forces, such as electrostatic and hydrophobic interactions, ionic and hydrogen bonds, van der Waals forces, or a combination of those, was selected for our new diagnostic platform.[25−27] The biofunctionalization protocol based on physical adsorption involves two main steps: the noncovalent and random immobilization of the antibodies and the blocking of the remaining free sites on the sensor surface to prevent nonspecific adsorptions.

To pursue the biosensing evaluation, an optimization with buffer is advised before using complex matrices, such as urine. The evaluation in buffer will allow us to study the performance of the biosensor platform for the specific TB biomarker without the interference of other proteins or compounds also present in urine.

Different immobilization parameters must be optimized for LAM detection in buffer. In order to provide a good anti-LAM density with enough accessibility to LAM and to guarantee a suitable surface coverage for minimizing nonspecific adsorptions, various concentrations of the antibody and BSA, as blocking agent, were tested to improve the immobilization performance. Each antibody concentration, ranging from 10 to 100 μg/mL, was evaluated at fixed conditions for pump speed (10 μL/min) and time (30 min). The surface coverage was analyzed from the immobilization signal. Immobilization signals showed an increasing tendency with increasing antibody concentrations (data not shown). As antibody concentrations above 50 μg/mL showed a similar signal, this means that the sensor surface was almost covered with 50 μg/mL of the antibody. After the antibody immobilization, the same procedure was followed for the blocking step using different concentrations of BSA (from 1 to 10 mg/mL) and analyzing the detection signal of a nonspecific protein (data not shown). A PBS 10 mM solution with 10 mg/mL of BSA was the one that blocks the remaining free sensor surface areas and avoids nonspecific adsorptions.

Using the optimized protocol, an antibody solution (50 μg/mL) in PBS 10 mM was injected followed by a BSA solution (10 mg/mL). Milli-Q water was employed as running buffer for the immobilization step. The immobilization step shows high reproducibility between different sensor cartridges (coefficient of variation (CV): 5%). The running buffer was changed to PBS 10 mM once the immobilization process was finished and the target detection was then carried out. Target LAM samples were dissolved in PBS 10 mM at concentrations ranging from 1 to 1000 ng/mL and injected into the system. All experiments with LAM in buffer were done by triplicate.

An example of real-time LAM detection (250 ng/mL) with the POC instrument is shown in Figure 4A. A simultaneous good response for all of the sensors contained in the same photonic sensor chip was observed.

As antibodies are not covalently attached to the sensor surface, it was not possible to regenerate the biosurface. For this reason, we have employed an additive immunoassay.

Successive dilutions of increasing LAM concentrations were injected in order to estimate the sensitivity, as shown in Figure 4B. For all of the concentrations evaluated, a clear sensor response was obtained. As expected with an additive assay, the antibody reaches a saturation level and loses its ability to detect more LAM, explaining the reduced sensor signal. For example, Figure 4B shows a higher LAM signal response for 250 ng/mL than for 1000 ng/mL.

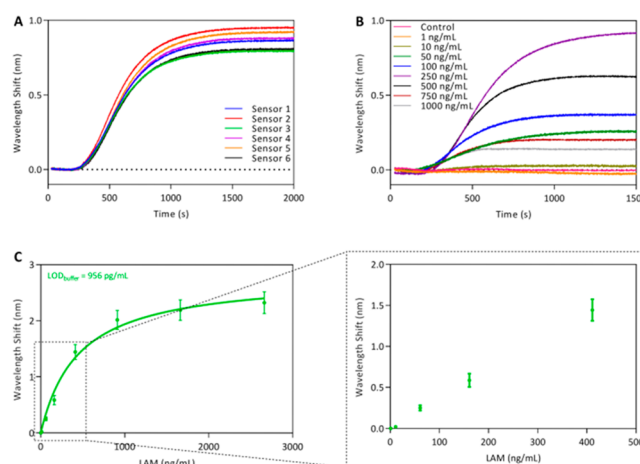The selectivity of the biosensor was tested under the explained conditions for LAM detection, monitoring the

Figure 4. (A) Real-time sensogram showing the detection of 250 ng/mL LAM in buffer. (B) Sensograms showing the LAM detection at different concentrations (from 1 to 1000 ng/mL LAM) in buffer. (C) Calibration curve obtained for different LAM concentrations in buffer. Solid line corresponds to the one-site specific binding fit. All data show mean ± SD of triplicate measurements.

wavelength shift after the injection of 1000 ng/mL of BSA protein, a nonspecific protein for the immobilized antibody. As observed in Figure 4B (control), BSA protein leads to a negligible response of the biosensor.

A calibration curve of triplicates for LAM detection in buffer was plotted in Figure 4C, resulting in a LOD of 956 pg/mL equivalent to 54.63 pM (R^2 = 0.98), revealing the excellent sensitivity of the sensors and the selectivity of the antibodies against LAM, and overall indicating the good performance of the photonic chip and the prototype instrument.

For the evaluation of the reproducibility between sensors, the standard deviation was calculated for nine different detection signals by triplicate, obtaining a mean value of 40 pm. This result demonstrates that the variability between sensors is negligible.

LAM Analysis in Spiked Urine Samples. The main goal for a sensor applied to clinical diagnosis is the ability to detect a biomarker or a panel of biomarkers associated with the disease directly in human biological fluids, preferably obtained using a noninvasive technique. For this reason, the next step in our study was the evaluation of LAM directly in human urine. Urine is an ideal candidate for a POC platform due to its advantages in obtainment and storage.

We directly analyzed LAM in real human urine samples, which is especially complex due to the undesired nonspecific adsorption of different urine components. Several blocking agents can be employed to avoid or greatly decrease nonspecific adsorption on the sensor surface. Previous studies have demonstrated that coating of the sensor surface with PLL-g-PEG and the presence of surfactant agent Tween 20 in the detection buffer, minimizes the background signal produced by undiluted urine.[28−30] Based on this, we have studied the effect of different concentrations of blocking agents in order to reduce nonspecific adsorption when flowing urine from a healthy patient over the sensors were we have previously immobilized the anti-LAM antibody: (i) 10 mg/mL BSA, (ii) 0.5 mg/mL PLL-g-PEG, and (iii) 0.75 mg/mL PLL-g-PEG and 10 mg/mL BSA. First, an undiluted urine sample from a healthy donor was injected on the surface blocked with 10 mg/mL BSA and resulted in a background signal of 1.27 nm.

Second, using 0.5 mg/mL PLL-*g*-PEG for the surface blocking, we observed a strong reduction of nonspecific binding of undiluted urine with respect to BSA solution, but we cannot consider it as a negligible signal. In order to avoid this small signal, a combination of 0.75 mg/mL PLL-*g*-PEG and 10 mg/mL BSA was used to minimize nonspecific adsorption between the urine components and the sensor surface to 80 pm. Thus, we will adopt this strategy for future evaluations of real urine samples and use PBS 10 mM with 0.5% of Tween 20 (PBST 0.5%) as the running buffer for the evaluation of urine samples. When monitoring undiluted urine in real-time, a peak can be observed when the sample starts to flow in the sensing area (see Figure 5B), which we attribute to the use of PBST 0.5% as running buffer.
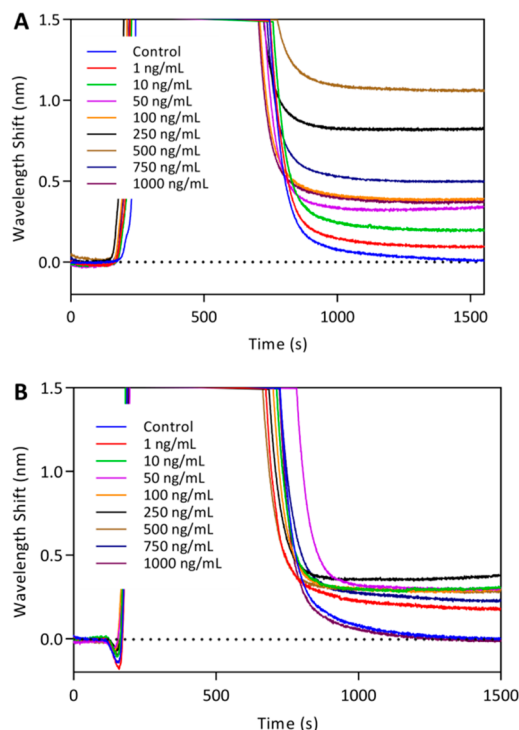

Figure 6. Calibration curves obtained for different LAM concentrations in buffer, diluted urine and undiluted urine. Solid line corresponds to the one-site specific binding fit of every curve. All data show mean ± standard deviation of triplicate measurements.

Figure 5. Sensograms showing the LAM detection at different concentrations (from 1 to 1000 ng/mL) and control in (A) diluted and (B) undiluted urine.

Diluted urine and undiluted urine were evaluated in order to observe possible interferences of the urine matrix in the additive assay. Spiked urine samples with different LAM concentrations were diluted 1:1 in PBS 20 mM or injected directly without a pretreatment onto the sensor. Figure 5 illustrates the different LAM concentrations in diluted and undiluted urine. Injection of urine from a healthy donor was performed, resulting in no background signal (see Figure 5) and confirming the absence of nonspecific adsorptions of urine components.

A calibration curve of triplicates for LAM-spiked diluted and undiluted is plotted in Figure 6, resulting in a LOD of 731 pg/mL (41.77 pM; R^2 = 0.97) and 475 pg/mL (27.14 pM; R^2 = 0.92), respectively. With reproducible and repetitive results, the curve of LAM-spiked undiluted urine showed higher sensitivity than in buffer and diluted urine (see Figure 6), suggesting that urine components create a more favorable environment for the antibody−antigen interaction. However,
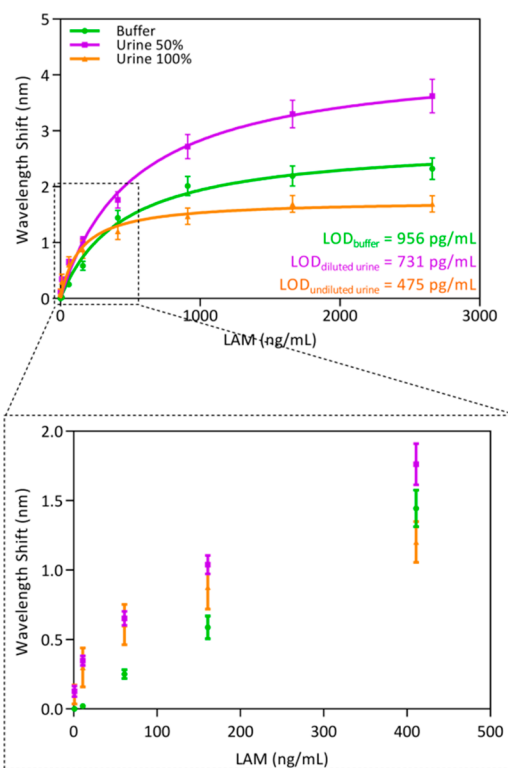
despite the high sensitivity obtained in undiluted urine, there is no definitive information about which one is the minimum concentration of LAM in urine of TB patients; some references reported minimum values about 100 and 200 pg/mL but the evaluation was done in a limited number of samples of TB patients (with and without HIV).[14,31] In the case that such low concentrations have to be reach, we will not achieve them with a direct immunoassay. For this reason, the use of a secondary antibody able to amplify the signal was foreseen in our project. For that, a third syringe was included in the sensor cartridge design (see Figure 2), which can be employed for the injection of the secondary antibody is required. This strategy was not finally needed in this work because all the evaluated samples from real patients contained higher LAM concentrations.

The LOD in undiluted urine obtained with our new POC platform is better than those achieved using commercial lateral flow tests (LOD 10^5−10^6 pM) and conventional ELISAs (LOD 1.83×10^5 pM), using different antibodies and immunoassay formats.[31−33]

The results confirmed the high sensitivity and specificity of our methodology, as well as the robustness of not only the antibodies but also the photonic sensor chips and the prototype instrument. In case that a positive signal is observed with this methodology, it would presumably represent the specific recognition of LAM by the antibodies immobilized on the sensor surface.

Validation with Real Urine Samples. With the promising previous results in spiked urine, we were able to validate the prototype using a direct assay without the need of any pretreatment of the human urine samples to be analyzed. There are some parameters, such as pH and the concentration

of different urine components, which can strongly vary between patients and which can have an effect in the evaluation.

With the optimal conditions previously selected for the evaluation of undiluted urine, we applied the POC platform to study the presence of LAM in the urine of 10 patients with confirmed TB from Tanzania and 10 healthy patients from Tanzania and Spain. The Tanzania samples were collected from hospitals and directly observed treatment short course (DOTS) centers,[34] while the Spain samples were donated by volunteers.

Nontreated and undiluted real urine samples were directly flowed over the photonic sensor chip using the in-flow system. Signals were monitored in real-time and converted into positive or negative TB diagnosis depending on the obtained LAM signal, as shown in Figure 7A. Based on the shifts from
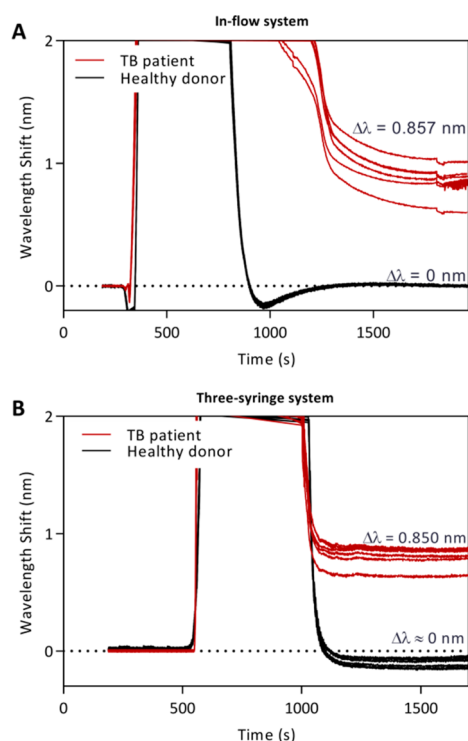

Figure 7. Real-time sensograms for the comparison of two real urine samples using (A) three-syringe and (B) in-flow systems.

the optimization process, patients were determined to be TB positive if the LAM signal was higher than 90 pm. Through evaluation of 20 real urine samples and taking into account this threshold, only one concentration in urine, due to the fact that LAM is a cell wall component of *M. tuberculosis* and can only be present in the urine of those infected with the pathogenic bacteria.

Positive results with the in-flow system allow the evaluation of the same real samples using the final configuration of the POC prototype which does not use the external pumps but employs a three-syringe system. With this configuration, two of the syringes contained PBST 0.5% and the other one the urine sample (150 μL). An example of a real-time signal for the same samples as for the in-flow system is shown in Figure 7B. The resulted signal for healthy urine returns back to the baseline (see Figure 7B).

A comparison between both systems for the evaluation of two specific samples is shown in Figure 7. With both systems, we cannot observe any significance difference in the absolute value of the obtained wavelength shift variation. This can also be observed in Figure 8 for the 20 urine samples analyzed. The
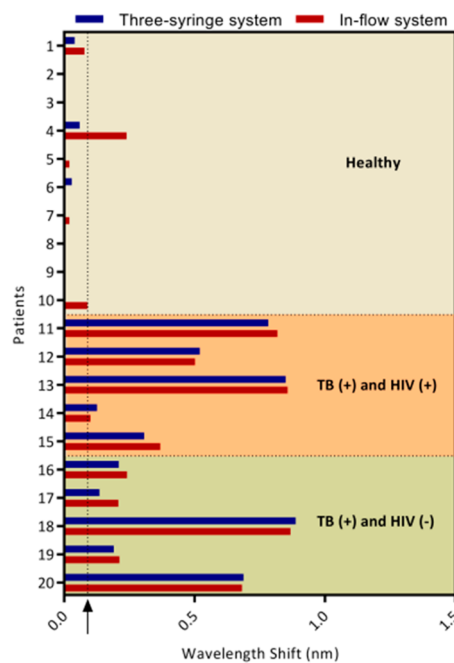

Figure 8. Bar plot of the wavelength shift signals obtained from the analysis of 20 urine samples from healthy and TB patients with and without HIV using two different systems for the fluid injection. Black arrow shows the threshold to classify patients as healthy or infected.

main difference between both systems was observed for Patient 4 (see Figure 8), who was the only false positive observed in our study when using the in-flow system. Taking account all these results, we can corroborate the high reproducibility and diagnosis capacity of our methodology.

One of the disadvantages of the current LAM detection methods in urine is that they are not able to detect TB in people without HIV. However, with our novel POC platform, the time to result is only 15 min for the classification of patients as healthy or infected, regardless of HIV coinfection, as shown in Figure 8.

Tables 1 and 2 list and compare the results of the analysis obtained with the novel POC and with current techniques such as GeneXpert and sputum smear microscopy. For each patient, the values of pH, HIV status, and current TB diagnosis are reported. Results obtained with our platform show a good correlation to those obtained with the current methods as observed when compared the data in both tables. As illustrated in Figure 8 and Tables 1 and 2, out of the 20 real urine samples analyzed by duplicate, 10 samples were true positive and 9 samples were true negative; and when using the in-flow approach, only one sample was a false positive. Therefore, the validation of the novel POC platform using the final configuration with three-syringe showed a sensitivity of 100%, a specificity of 100% and an area under the curve (AUC) of 1 as calculated by a ROC curve analysis (Figure S-4). This analysis was also carried out for the in-flow system and both systems together (Figures S-5 and S-6).

Table 1. Evaluation of Urine Samples from Healthy Volunteers with the POC Prototype

Healthy donors	pH	POC prototype	
		Three-syringe	In-flow
1	8	no	no
2	8	no	no
3	8	no	no
4	7	no	yes
5	7	no	no
6	7	no	no
7	8	no	no
8	9	no	no
9	8	no	no
10	6	no	no

Table 2. Evaluation of Urine Samples from Patients with Confirmed TB Using Current Methodologies (GeneXpert and Microscopy) in Comparison with the POC Prototype[a]

P	HIV	TB	pH	Current methods		POC prototype	
				T1	T2	Three-syringe	In-flow
11	0	yes	8	N/A	N/A	yes	yes
12	1	yes	8	N/A	N/A	yes	yes
13	1	yes	8	N/A	N/A	yes	yes
14	1	yes	7	yes	no	yes	yes
15	0	yes	7	yes	yes	yes	yes
16	0	yes	7	yes	yes	yes	yes
17	0	yes	8	yes	yes	yes	yes
18	1	yes	9	yes	yes	yes	yes
19	1	yes	8	yes	yes	yes	yes
20	0	no	6	N/A	N/A	yes	yes

[a]P, patients; HIV, HIV status; TB, TB diagnosis; T1, GeneXpert; T2, microscopy.

CONCLUSIONS

We have developed a novel POC platform for the detection of a cell wall component of *M. tuberculosis* in undiluted urine based on a highly sensitive MZI sensor chip integrated in a polymer microfluidic cartridge. The strategy consists of a direct immunoassay for the label-free LAM detection in unprocessed urine previously immobilizing by physical adsorption a specific monoclonal antibody. Several parameters have been optimized and an additive immunoassay has been selected as a proof-of-concept for the evaluation of our novel POC platform, reaching a limit of detection as low as 475 pg/mL (27.14 pM) for the direct detection in spiked urine samples and corroborating the excellent selectivity and sensitivity of the produced antibodies. We are now in the process of optimization of a biofunctionalization protocol for the covalent binding of the antibodies to allow surface regeneration during laboratory testing and leave aside some drawbacks of additive immunoassays.

The validation of the methodology with clinical samples from TB patients and healthy donor samples allows the detection of TB in people with and without HIV coinfection, and the results show excellent correlation to those obtained with GeneXpert and sputum microscopy techniques. The platform has shown a high sensitivity (100%) and specificity (100%) in comparison with rapid tests commercially available for TB detection. The diagnosis of people only infected with TB has not been possible with the current rapid tests on the market, providing more advantages to our POC instrument. The advantages added to our instrument (low cost, single-use, user friendliness, results in 15 min, no requirement for qualified personnel for operation, and no need of special laboratory infrastructure) make this POC platform an outstanding candidate for in situ use in a primary doctor's office and patient's bedsides. We therefore demonstrated the high sensitivity, specificity, and applicability of our platform, which could be used during routine check-ups in developing countries.

As the instrument is designed for the simultaneous detection of a panel of six different biomarkers, this opens the door for the use of our POC platform for the fast detection of different diseases, such as diabetes, cancer, HIV, stroke, heart diseases, dementias diseases, malaria, hepatitis A, respiratory infections, and kidney diseases, among others.

ASSOCIATED CONTENT

Ⓢ Supporting Information

The Supporting Information is available free of charge on the ACS Publications website at DOI: 10.1021/acssensors.8b00393.

> Additional text and figures showing the reagents, ethics statement, data analysis and complete prototype instrument, as well as further description of the monoclonal antibody and target production, studying the affinity and providing kinetics properties of the monoclonal antibody; Receiver Operating Characteristic (ROC) analysis for the diagnostic performance of our platform (PDF)

AUTHOR INFORMATION

Corresponding Author

*E-mail: laura.lechuga@icn2.cat.

ORCID Ⓞ

Laura M. Lechuga: 0000-0001-5187-5358

Author Contributions

The manuscript was written through contributions of all authors. All authors have given approval to the final version of the manuscript.

Notes

The authors declare no competing financial interest.

REFERENCES

(1) WHO. *Global Tuberculosis Report 2017*; 2017.

(2) Srivastava, S. K.; van Rijn, C. J. M.; Jongsma, M. A. Biosensor-Based Detection of Tuberculosis. *RSC Adv.* **2016**, *6* (22), 17759–17771.

(3) Pai, M.; Behr, M. A.; Dowdy, D.; Dheda, K.; Divangahi, M.; Boehme, C. C.; Ginsberg, A.; Swaminathan, S.; Spigelman, M.; Getahun, H. Tuberculosis. *Nat. Rev. Dis. Prim.* **2016**, *2*, 1–23.

(4) Shah, M.; Chihota, V.; Coetzee, G.; Churchyard, G.; Dorman, S. E. Comparison of Laboratory Costs of Rapid Molecular Tests and Conventional Diagnostics for Detection of Tuberculosis and Drug-

Resistant Tuberculosis in South Africa. *BMC Infect. Dis.* **2013**, *13* (1), 1−8.

(5) Callaway, E. Improved Diagnostics Fail to Halt the Rise of Tuberculosis. *Nature* **2017**, *551* (7681), 424−425.

(6) Viñuelas-Bayón, J.; Vitoria, M. A.; Samper, S. Rapid Diagnosis of Tuberculosis. Detection of Drug Resistance Mechanisms. *Enfermedades Infecc. y Microbiol. Clin. (English ed.)* **2017**, *35* (8), 520−528.

(7) Goletti, D.; Petruccioli, E.; Joosten, S. A.; Ottenhoff, T. H. M. Tuberculosis Biomarkers: From Diagnosis to Protection. *Infect. Dis. Rep.* **2016**, *8* (2), 24−32.

(8) Dheda, K.; Barry, C. E.; Maartens, G. Tuberculosis. *Lancet* **2016**, *387* (10024), 1211−1226.

(9) Bekmurzayeva, A.; Sypabekova, M.; Kanayeva, D. Tuberculosis Diagnosis Using Immunodominant, Secreted Antigens of Mycobacterium Tuberculosis. *Tuberculosis* **2013**, *93* (4), 381−388.

(10) Woldeyohannes, D.; Sisay, S.; Mengistu, B.; Kassa, H. Directly Observed Treatment Short-Course (DOTS) for Treatment of New Tuberculosis Cases in Somali Regional State, Eastern Ethiopia: Ten Years Retrospective Study. *BMC Res. Notes* **2015**, *8* (1), 1−7.

(11) Shete, P. B.; Ravindran, R.; Chang, E.; Worodria, W.; Chaisson, L. H.; Andama, A.; Davis, J. L.; Luciw, P. A.; Huang, L.; Khan, I. H. Evaluation of Antibody Responses to Panels of M. Tuberculosis Antigens as a Screening Tool for Active Tuberculosis in Uganda. *PLoS One* **2017**, *12* (8), 1−12.

(12) Montoya, A.; March, C.; Montagut, Y.; Moreno, M.; Manclus, J.; Arnau, A.; Jimenez, Y.; Jaramillo, M.; Marin, P.; Torres, R. A High Fundamental Frequency (HFF)-Based QCM Immunosensor for Tuberculosis Detection. *Curr. Top. Med. Chem.* **2017**, *17* (14), 1623−1630.

(13) Peter, J.; Green, C.; Hoelscher, M.; Mwaba, P.; Zumla, A.; Dheda, K. Urine for the Diagnosis of Tuberculosis: Current Approaches, Clinical Applicability, and New Developments. *Curr. Opin. Pulm. Med.* **2010**, *16* (3), 262−270.

(14) Hamasur, B.; Bruchfeld, J.; Haile, M.; Pawlowski, A.; Bjorvatn, B.; Källenius, G.; Svenson, S. B. Rapid Diagnosis of Tuberculosis by Detection of Mycobacterial Lipoarabinomannan in Urine. *J. Microbiol. Methods* **2001**, *45* (1), 41−52.

(15) World Health Organization. *The Use of Lateral Flow Urine Lipoarabinomannan Assay (LF-LAM) for the Diagnosis and Screening of Active Tuberculosis in People Living with HIV: Policy*; 2015; pp 1−74.

(16) Agha, M. A.; El-Helbawy, R. H.; El-Helbawy, N. G.; El-Sheak, N. M. Utility of Quantitative Analysis of Urine Lipoarabinomannan in the Diagnosis of Tuberculosis. *Egypt. J. Chest Dis. Tuberc.* **2013**, *62* (3), 401−407.

(17) Minion, J.; Leung, E.; Talbot, E.; Dheda, K.; Pai, M.; Menzies, D. Diagnosing Tuberculosis with Urine Lipoarabinomannan: Systematic Review and Meta-Analysis. *Eur. Respir. J.* **2011**, *38* (6), 1398−1405.

(18) Mukundan, H.; Price, D. N.; Goertz, M.; Parthasarathi, R.; Montaño, G. A.; Kumar, S.; Scholfield, M. R.; Anderson, A. S.; Gnanakaran, S.; Iyer, S. Understanding the Interaction of Lipoarabinomannan with Membrane Mimetic Architectures. *Tuberculosis* **2012**, *92* (1), 38−47.

(19) Mishra, A. K.; Driessen, N. N.; Appelmelk, B. J.; Besra, G. S. Lipoarabinomannan and Related Glycoconjugates: Structure, Biogenesis and Role in Mycobacterium Tuberculosis Physiology and Host-Pathogen Interaction. *FEMS Microbiol. Rev.* **2011**, *35* (6), 1126−1157.

(20) Fukuda, T.; Matsumura, T.; Ato, M.; Hamasaki, M.; Nishiuchi, Y.; Murakami, Y.; Maeda, Y.; Yoshimori, T.; Matsumoto, S.; Kobayashi, K. Critical Roles for Lipomannan and Lipoarabinomannan in Cell Wall Integrity of Mycobacteria and Pathogenesis of Tuberculosis. *mBio* **2013**, *4* (1), 8−10.

(21) Paris, L.; Magni, R.; Zaidi, F.; Araujo, R.; Saini, N.; Harpole, M.; Coronel, J.; Kirwan, D. E.; Steinberg, H.; Gilman, R. H. Urine Lipoarabinomannan Glycan in HIV-Negative Patients with Pulmonary Tuberculosis Correlates with Disease Severity. *Sci. Transl. Med.* **2017**, *9*, 1−12.

(22) Lawn, S. D. Point-of-Care Detection of Lipoarabinomannan (LAM) in Urine for Diagnosis of HIV-Associated Tuberculosis: A State of the Art Review. *BMC Infect. Dis.* **2012**, *12* (1), 1−12.

(23) Martens, D.; Ramirez-Priego, P.; Murib, M. S.; Elamin, A. A.; Gonzalez-Guerrero, A. B.; Stehr, M.; Jonas, F.; Anton, B.; Hlawatsch, N.; Soetaert, P. A Low-Cost Integrated Biosensing Platform Based on SiN Nanophotonics for Biomarker Detection in Urine. *Anal. Methods* **2018**, *10* (25), 3066−3073.

(24) González-Guerrero, A. B.; Maldonado, J.; Herranz, S.; Lechuga, L. M. Trends in Photonic Lab-on-Chip Interferometric Biosensors for Point-of-Care Diagnostics. *Anal. Methods* **2016**, *8* (48), 8380−8394.

(25) Welch, N. G.; Scoble, J. A.; Muir, B. W.; Pigram, P. J. Orientation and Characterization of Immobilized Antibodies for Improved Immunoassays (Review). *Biointerphases* **2017**, *12* (2), 02D301.

(26) Kim, D.; Herr, A. E. Protein Immobilization Techniques for Microfluidic Assays. *Biomicrofluidics* **2013**, *7* (4), 041501.

(27) Trilling, A. K.; Beekwilder, J.; Zuilhof, H. Antibody Orientation on Biosensor Surfaces: A Minireview. *Analyst* **2013**, *138* (6), 1619−1627.

(28) Soler, M.; Estevez, M.-C.; Villar-Vazquez, R.; Casal, J. I.; Lechuga, L. M. Label-Free Nanoplasmonic Sensing of Tumor-Associate Autoantibodies for Early Diagnosis of Colorectal Cancer. *Anal. Chim. Acta* **2016**, *930*, 31−38.

(29) Gutiérrez-Mejía, F. A.; van Ijzendoorn, L. J.; Prins, M. W. J. Surfactants Modify the Torsion Properties of Proteins: A Single Molecule Study. *New Biotechnol.* **2015**, *32* (5), 441−449.

(30) Soler, M.; Estevez, M.-C.; Alvarez, M.; Otte, M. A.; Sepulveda, B.; Lechuga, L. M. Direct Detection of Protein Biomarkers in Human Fluids Using Site-Specific Antibody Immobilization Strategies. *Sensors* **2014**, *14* (2), 2239−2258.

(31) Mukundan, H.; Kumar, S.; Price, D. N.; Ray, S. M.; Lee, Y. J.; Min, S.; Eum, S.; Kubicek-Sutherland, J.; Resnick, J. M.; Grace, W. K. Rapid Detection of Mycobacterium Tuberculosis Biomarkers in a Sandwich Immunoassay Format Using a Waveguide-Based Optical Biosensor. *Tuberculosis* **2012**, *92* (5), 407−416.

(32) Shah, M.; Variava, E.; Holmes, C. B.; Coppin, A.; Golub, J. E.; McCallum, J.; Wong, M.; Luke, B.; Martin, D. J.; Chaisson, R. E. Diagnostic Accuracy of a Urine Lipoarabinomannan Test for Tuberculosis in Hospitalized Patients in a High HIV Prevalence Setting. *JAIDS, J. Acquired Immune Defic. Syndr.* **2009**, *52* (2), 145−151.

(33) Shah, M.; Martinson, N. A.; Chaisson, R. E.; Martin, D. J.; Variava, E.; Dorman, S. E. Quantitative Analysis of a Urine-Based Assay for Detection of Lipoarabinomannan in Patients with Tuberculosis. *J. Clin. Microbiol.* **2010**, *48* (8), 2972−2974.

(34) WHO. World Health Organization. What Is DOTS (Directly Observed Treatment, Short Course)? *SEARO*, 2017.